



EFFECT OF SIGNAL MODULATION OF DBD PLASMA ACTUATOR ON FLOW CONTROL AROUND NACA 0015

Adem Arif GÜLER*, Mehmet SEYHAN** and Yahya Erkan AKANSU***

Niğde Ömer Halisdemir University, Mechanical Engineering Department
51240, Niğde, *ademarifguler@hotmail.com, ***akansu@ohu.edu.tr

**Karadeniz Technical University, Mechanical Engineering Department
61080, Trabzon, mehmetseyhan@ktu.edu.tr

(Geliş Tarihi: 26.09.2017, Kabul Tarihi: 20.04.2018)

Abstract: Effects of DBD plasma actuator driven by six different type modulated signals on flow around NACA 0015 airfoil are experimentally investigated for lift augmentation. One actuator attached to the upside of the airfoil at $x/c = 0.1$ is used. Force measurement and smoke wire flow visualization are performed in a low speed wind tunnel. For $Re = 3.6 \times 10^4$, the actuator is driven with six different signal modulations among which frequency modulation, amplitude modulation, excitation frequency and duty cycle at $\alpha = 10^\circ$. SM4 including amplitude modulation is indicated to have better performance than the other signal modulations. Signal modulations provide energy savings while generating plasma to increase the lift coefficient. The obtained results indicate that as the dimensionless excitation frequency (F^+) is 1 at low duty cycle, a better lift coefficient is obtained in comparison with the other F^+ values. For $Re = 3 \times 10^4$, the lift coefficient is proportionally increased with driving voltage and frequency due to increasing induced flow at $\alpha = 10^\circ$. Flow visualization results showed that the separated shear layer at the leading edge gets closer to the (suction) surface of the airfoil by increasing the driving voltage from 6 kV_{pp} to 8 kV_{pp} which confirms the driving voltage effect.

Keywords: Airfoil, Signal modulation, Active flow control, DBD plasma actuator.

DBD PLAZMA EYLEYİCİSİ SİNYAL MODÜLASYONUNUN NACA 0015 ETRAFINDAKİ AKIŞ KONTROLÜNE ETKİSİ

Özet: NACA 0015 uçak kanadı etrafındaki akış üzerine altı farklı tipte sinyalle sürülen DBD plazma eyleyicisinin etkileri kaldırma kuvvetinin artırılması için deneysel olarak incelenmiştir. Uçak kanadının $x/c = 0.1$ konumuna yerleştirilen tek eyleyici kullanılmıştır. Kuvvet ölçümü ve duman tek akış görüntülemesi düşük hızlı bir rüzgar tüneline gerçekleştirilmiştir. Frekans modülasyonu, genlik modülasyonu, uyarım frekansı ve doluluk boşluk oranını içeren altı farklı sinyalle $Re = 3.6 \times 10^4$ için $\alpha = 10^\circ$ 'da eyleyici sürülmüştür. Genlik modülasyonu içeren SM4 diğer sinyal modülasyonlarından daha iyi performans göstermiştir. Sinyal modülasyonu, kaldırma kuvvetini arttırmak için plazma üretirken enerji tasarrufu sağlayabilir. Elde edilen sonuçlar, boyutsuz uyarım frekansı (F^+) düşük doluluk boşluk oranı $F^+ = 1$ 'deyken, en iyi kaldırma katsayısının diğer F^+ değerleriyle karşılaştırıldığında elde edildiğini göstermiştir. $Re = 3 \times 10^4$ için kaldırma katsayısı, sürüm voltajı ve frekansıyla orantılı bir şekilde $\alpha = 10^\circ$ derecede eyleyici hızının artmasından dolayı artmıştır. Akış görüntüleme sonuçları, hücum kenarında ayrılmış kayma tabakasının sürüm voltajının 6 kV_{pp}'dan 8 kV_{pp}'a artmasıyla uçak kanadının yüzeyi üzerine yaklaşması sürüm voltajının etkisini doğrulamaktadır.

Anahtar Kelimeler: Uçak kanadı, Sinyal modülasyonu, Aktif akış kontrolü, DBD plazma eyleyici.

SEMBOLLER VE KISALTMALAR

F^+	Dimensionless excitation frequency
f_e	Excitation frequency, [Hz]
f_{RF}	Driven signal radio frequency, [kHz]
U_∞	Free stream velocity, [m/s]
C_L	Lift coefficient
x	Distance from leading edge to actuator, [m]
c	Chord length, [m]
α	Attack angle, [$^\circ$]
Re	Reynolds number
ν	Kinematic viscosity, [m ² /s]
ρ	Density, [kg/m ³]
$F_{x,y \text{ and } z}$	x, y and z axis force, [N]
$T_{x,y \text{ and } z}$	x, y and z axis torque, [Nm]
V	Driving voltage, [kV _{pp}]

AFC	Active flow control
AM	Amplitude modulation
DBD	Dielectric barrier discharge
EHD	Electrohydrodynamic
PFC	Passive flow control
PM	Pulse modulation
SM	Signal modulation
UAVs	Unmanned aerial vehicles

INTRODUCTION

Flow control is important to improve the flow characteristic around bluff bodies and aerodynamic shaped bodies. In order to manipulate the flow, there are some active and passive flow control methods which are

used together with different devices. The passive flow control (PFC) methods do not need an energy input since only geometric modifications to the bluff and/or aerodynamic shaped body is made. Spoilers (Akansu *et al.*, 2016), Splitter plates (Akansu *et al.*, 2004; Sarioglu, 2016; Sarioglu *et al.*, 2006), control rods (Sarioglu *et al.*, 2005) amongst others can be given as examples of geometric modifications. Active flow control (AFC) requires different forms of energy inputs to produce plasma, acoustic wave or heat, for example to acquire the desired effects such as drag reduction (Akbiyik *et al.*, 2017), lift augmentation (Asada *et al.*, 2009; Little *et al.*, 2010; Taleghani *et al.*, 2012) and vortex shedding suppression (Thomas *et al.* 2008).

In AFC methods, flow control based on plasma is classified as Magnetohydrodynamic (MHD) which means a flow field is imposed magnetically and electrohydrodynamic (EHD) where the flow field is influenced electrically producing ion wind. A dielectric barrier discharge (DBD) plasma actuator known as one of EHD methods has taken attention by researcher around the whole world due to its low mass, fast response time, easy integration into the system without additional cavities or holes, and lack of moving parts (Corke *et al.* 2009). The induced flow velocity of a single DBD plasma actuator reaches up to 7 m/s (Benard and Moreau 2014; Forte *et al.* 2007). Therefore this actuator is effective to control the flow at low Reynolds number and high angles of attack (Benard and Moreau 2011; Moreau 2007). Improvement of aerodynamic performance of airfoils working at low Reynolds numbers could help to solve the problems for high altitude remotely piloted vehicles, slow flying unmanned aerial vehicles (UAVs), micro air vehicles (MAVs) (Genç *et al.* 2012; Rudmin *et al.* 2013; Sosa and Artana 2006), jet engine fan blades, wind turbine rotors and propellers at high altitude (Sosa and Artana 2006).

Airfoil flow regime at low Reynolds number suffer from some aerodynamic phenomena like laminar separation, bubble formation and vortex shedding (Genç *et al.* 2012; Rudmin *et al.* 2013). The DBD plasma actuator located at the leading edge of the airfoil affects flow inside the boundary layer by adding momentum close to the wall. Therefore this leads to reattachment or flow of the separated shear layer close the surface of the airfoil (Benard and Moreau 2011; Esfahani *et al.* 2016). This actuator has wide application areas such as UAVs for separation control (Nelson *et al.* 2007; Patel *et al.* 2007), MAVs for flow control (Göksel *et al.* 2007; Greenblatt *et al.* 2008; Menghu *et al.* 2015), low pressure turbine for separation control (De Giorgi *et al.* 2017; Huang *et al.* 2006; Pescini *et al.* 2017). More extensive information about underlying physics and working principle of the DBD plasma actuator could be found in the review studies of Benard and Moreau (2014), Corke *et al.* (2009) and Wang *et al.* (2013)

Feng *et al.* (2012) investigated the effect of a DBD plasma actuator which is mounted to a gurney flap on the flow control over NACA0012 airfoil. The plasma actuator was driven by a sinusoidal signal at high AC voltage and

frequency. They indicated that the lift coefficient is increased when DBD plasma actuator is activated. According to velocity distribution, wake region with the gurney flap using the actuator is bigger than that of airfoil without the gurney flap. This situation means an augmentation in the lift coefficient of the airfoil. Asada *et al.* (2009) conducted a research on the influence of duty cycle of DBD plasma actuator on flow around NACA 0015 airfoil for Reynolds number between 44000 and 63000 in order to obtain lift augmentation and separation control. Their results show that smaller duty cycle values provide better flow separation control.

Little *et al.* (2010) investigated flow separation control over an EET high-lift airfoil with flap by using a DBD plasma actuator at Reynolds number up to 2.4×10^4 . Their results indicated that the amplitude signal modulation for a sinusoidal signal of DBD plasma actuator has less effect than duty cycle signal modulation for 30%, 50% and 70% of the duty cycle at the low frequencies. Akansu *et al.* (2013) researched the effect of DBD plasma actuator on NACA 0015 airfoil with respect to flow separation control and lift augmentation. Four DBD plasma actuators, mounted on $x/c = 0.1, 0.3, 0.5$ and 0.9 , were used by driving a continuous sinusoidal signal at $Re = 30500$. Their experimental parameters were $f_c = 17$ Hz and 100 Hz with driving voltage of 7 kV_{pp} at $\alpha = 12^\circ$ for the duty cycle case. An experimental study was conducted to investigate the piezoelectric and peristaltic EHD effect of DBD plasma actuator on the flow around NACA 0015 airfoil by Roth (2003). He also showed that the separated shear layer reattached onto the downstream surface of the airfoil in case 8 DBD actuators are used at attack angle up to 12° .

Taleghani *et al.* (2012) investigated the influence of duty cycle on the flow around a NLF0414 airfoil. They mounted a DBD plasma actuator on the airfoil surface, in three different locations at attack angles between 16° and 20° for Reynolds number of 7.5×10^5 . They performed all experiments using the sinusoidal signal at a voltage of 14 kV_{pp} and frequency of 28 kHz. Their results showed that lift augmentation at attack angle of 18° is higher than those in the other conditions at lower driving frequencies with lower duty cycles. Jukes *et al.* (2012) implemented an experimental study by using both a DBD plasma actuator and a Fiber Bragg Grating (FBG) sensor, which is used to determine flow separation, for flow separation control over NACA0024 airfoil at Reynolds number of 53000. The plasma actuator was supplied a voltage of 8 kV_{pp} and frequency of 9 kHz. They showed that the separated shear layer can reattach until an attack angle of 16° and maximum drag reduction (71%) is obtained at an attack angle of 12° . Moreover, particle image velocimetry was used to determine the flow field around the airfoil.

Asada *et al.* (2009), Taleghani *et al.* (2012) and Patel *et al.* (2008) reported that effectiveness of the DBD plasma actuator in terms of controlling flow separation and improving aerodynamic properties can be expressed by using the dimensionless excitation frequency which is defined as;

$$F^+ = \frac{f_e c}{U_\infty} \quad (1)$$

Here, F^+ is the dimensionless excitation frequency of the DBD plasma actuator, f_e is the excitation frequency of the DBD plasma actuator, c is the chord length of the airfoil and U_∞ is the free stream velocity of air.

Patel *et al.* (2008) and Göksel *et al.* (2007) showed that a DBD plasma actuator has the best effect in lift augmentation and the flow separation control on the flow around the airfoil at $F^+ = 1$ at a low duty cycle. However, Asada *et al.* (2009) showed that the best performance was measured at $F^+ = 9.1$ in contrast to Patel *et al.* (2008) and Göksel *et al.* (2007). According to this literature, there are two different results about the effect of the dimensionless excitation frequency so Taleghani *et al.* (2012) investigated the relation between F^+ and the duty cycle. They found that the optimum dimensionless excitation frequency increases when the duty cycle augments.

Signal modulations including frequency and amplitude modulation with/without duty cycle are studied by Benard and Moreau (2013), Little *et al.* (2010) and Daud *et al.* (2015). In the investigation of Benard and Moreau (2013), amplitude and burst modulation for DBD actuator excitation is used on the flow around a circular cylinder. These modulations increased the drag of the cylinder. Another study related to the signal modulation that consists of pulse modulation (PM) and amplitude modulation (AM) is performed by Daud *et al.* (2015). PM+AM case increases the lift coefficient on the flow around NACA 0015, where the actuator was placed at $x/c = 0.025$, when compared with PM case.

The most effective way to increase the efficiency of the single DBD plasma actuator is to improve this actuator performance by optimizing the actuator driving signal modulation without increasing its power consumption (Pescini *et al.* 2017). Therefore the present study focuses on four different amplitude modulation and five different dimensionless excitation frequencies with different duty cycle ratios. The main aim of this study is to investigate the effects of signal modulation on parameters such as the dimensionless excitation frequency, duty cycle and amplitude modulation of the DBD plasma actuator.

Experiments for this study are organized as follows. Firstly, lift coefficient variation versus attack angle is presented in order to compare results with the literature. Secondly, the variation of lift coefficient in wide Reynolds number range is investigated to determine the optimum Reynolds number which can be used in subsequent signal modulation study for three different attack angles and driving voltage. Variation of lift coefficient, based on driving voltage and frequency, and also smoke wire flow visualization is given at $Re = 3 \times 10^4$ and $\alpha = 10^\circ$. Thirdly, results of signal modulation and dimensionless excitation frequencies is presented at $Re = 3.6 \times 10^4$ and $\alpha = 10^\circ$.

EXPERIMENTAL SETUP

The experimental study is carried out in an open-type low speed wind tunnel having a square cross-section 57 cm x 57 cm in the Aerodynamic Flow Control Laboratory of Mechanical Engineering Department at Niğde Ömer Halisdemir University. The test section of the wind tunnel consists of plexiglass and has a divergence angle of 0.3 degrees to keep the static pressure constant between the test section inlet and outlet. Free-stream turbulence intensity is about 0.5 % in the working Reynolds number range.

The plasma actuator breaking down oxygen in the air with high voltage produces ozone gas. This gas is transferred to the outside of the laboratory by a PVC hose, connected to the wind tunnel, so that this gas does not harm human health. NACA 0015 airfoil has a chord length (c) of 150 mm and a spanwise length of 570 mm. Both the airfoil, that is made of ABS material, and end plates having 280 mm diameter are assembled so as to eliminate 3-dimensionality end effects. The distance between them is kept at 500 mm. Blockage ratios in the test section depend on the attack angle are 4%, 4.6% and 6.4% at $\alpha = 0^\circ, 10^\circ$ and 14° , respectively.

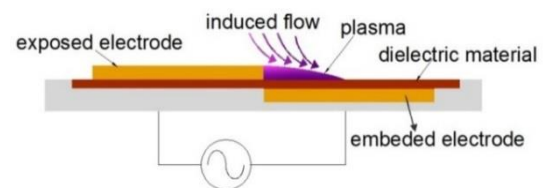


Figure 1. Schematic view of a DBD plasma actuator.

The DBD plasma actuator consists of two copper electrodes (one is an exposed electrode, the other is an embedded electrode) separated by Kapton tape as a dielectric material. A schematic view of the DBD plasma actuator is given in fig. 1. The exposed and embedded electrodes are 5 mm wide. The thicknesses of the electrode and Kapton dielectric are 0.05 mm and 0.07 mm, respectively. In this study, the thickness of the DBD plasma actuator of about 0.05 mm is created on the surface of the airfoil because the whole surface of the airfoil is covered with Kapton. As indicated by Akbıyık *et al.* (2016), the thickness of the actuator did not affect the flow inside the boundary layer like trip wire. When AC high voltage is applied between these electrodes, plasma as ionized air is produced.

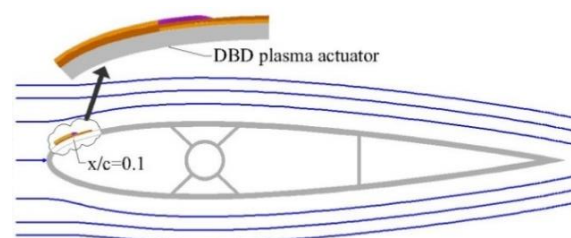


Figure 2. Schematic view of NACA 0015 airfoil model with DBD plasma actuator.

As shown in figure 2, one actuator is attached to the surface of the airfoil at $x/c=0.1$ in order to control the flow separation which strongly influences the lift force. It was chosen due to its optimal location to control the flow separation at the leading edge as suggested by Ibrahimoglu *et al.* (2016) and Post and Corke (2004). The airfoil, having a spanwise length of 500 mm, is covered with the actuator between the end plates. Smoke wire flow visualization is carried out at $Re = 3 \times 10^4$. Smoke lines are lightened with a cold light source. Pictures are captured with a digital camera.

The airfoil (shown in Fig 3) is horizontally centred on the test section and also is attached to a six axes ATI Gamma DAQ F/T load cell having three force axes: F_x , F_y , F_z and three torque components: T_x , T_y , T_z . Force can be measured up to $\pm 32N$ for x and y -axis directions. Force along the z axis can be also measured up to $\pm 100N$. This test model is connected to ISEL ZD30 rotary unit which is used under the load cell in order to rotate the airfoil in clockwise direction. ATI's F/T load cell largely eliminates crosstalks between the different measurement axes so as to obtain a precision measurement. The load cell was prepared to do instantaneous lift measurement (F_y).

Uncertainty of the measurements was computed with an uncertainty method suggested by Coleman and Steele (2009). Lift coefficient uncertainty including uncertainty of lift force, density, velocity and planform area was calculated to be 7%. Measurement data is collected at a sample rate of 300 Hz during 10 seconds in order to ensure enough data for accurate measurement. In addition, all experiments have been repeated thrice so as to verify the results. Figure 3 shows a 3D schematic view of the experimental setup which comprises of the load cell with the rotary unit, the airfoil within the test section,

an axis traverse, a micromanometer, a pitot tube, a high voltage power supply, an oscilloscope, a traverse controller and two computers. Free stream velocity (U_∞) was measured with the help of ManoAir 500 micromanometer that is connected to the pitot tube.

The electrical components of the experimental setup consist of a Trek 20/20C-HS high voltage power amplifier, a Tektronix TDS2022B model oscilloscope, a Fluke 80i-110s AC/DC current probe and a Tektronix P6015A high voltage probe. Disruptive voltage and the current were monitored with an oscilloscope using the high voltage probe and a current probe. The modulated signal of applied high voltage power supply was created by NI PCIe-7841R card via devoted software having four channels that generated a different waveform, duty cycle, time delay and the phase difference in LabVIEW software. The software interface is shown in figure 4. The fifth channel can be used for addition, subtraction, multiplication and division calculations for the other channels.

As illustrated in figure 5, the DBD actuator is driven by different modulated signals in order to produce the plasma in the flow separation region. SM1, SM2 etc. denote first signal modulation, second signal modulation etc. respectively. It is clear that this signal modification contains amplitude modification, duty cycle and frequency modification except for SM1 that is a continuous sinusoidal signal. Effects of these type signal modulations on the flow separation point are investigated in terms of effectiveness and energy consumption reduction. The effect of the DBD plasma actuator over the airfoil is investigated depending on the variation of Reynolds number that is smaller than $Re=1 \times 10^5$

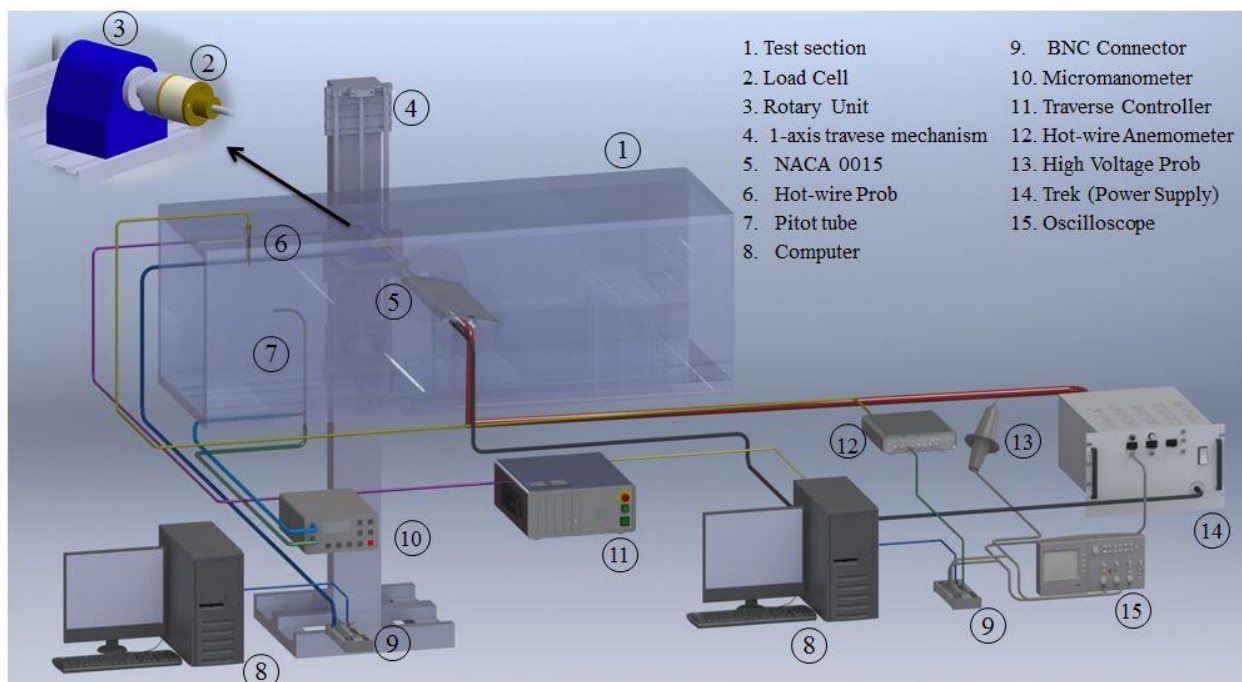


Figure 3. 3D schematic view of the experimental setup.

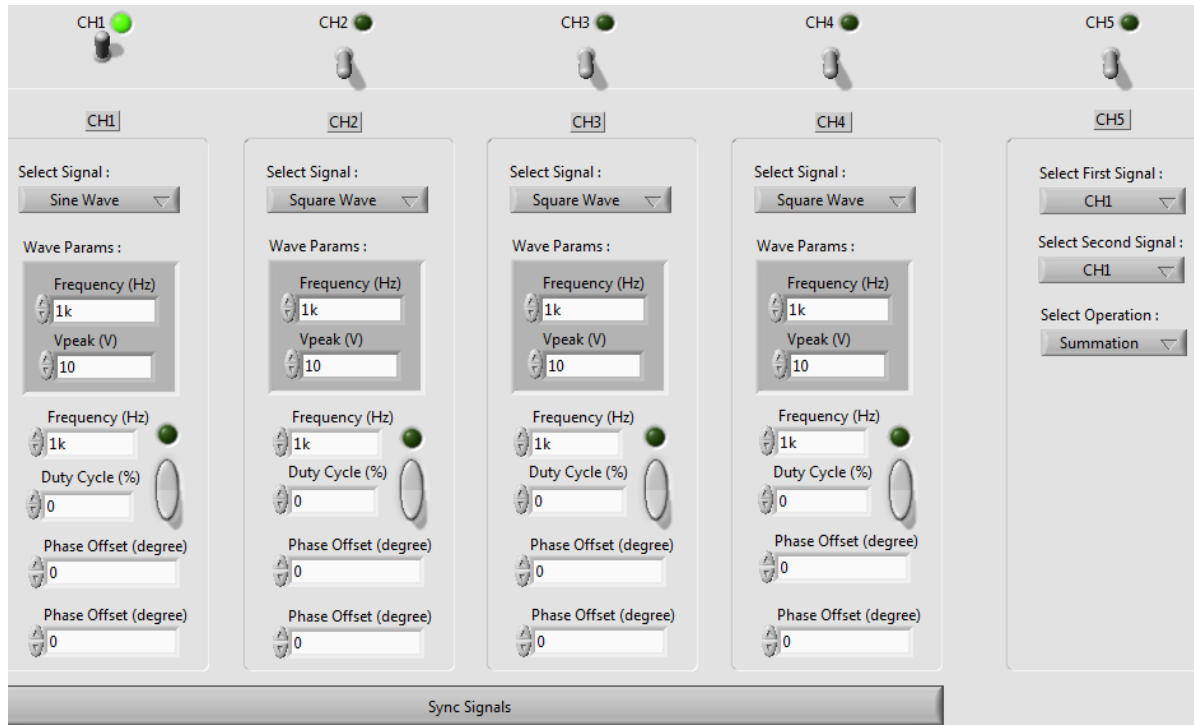


Figure 4. Developed software in order to generate signal modulation.

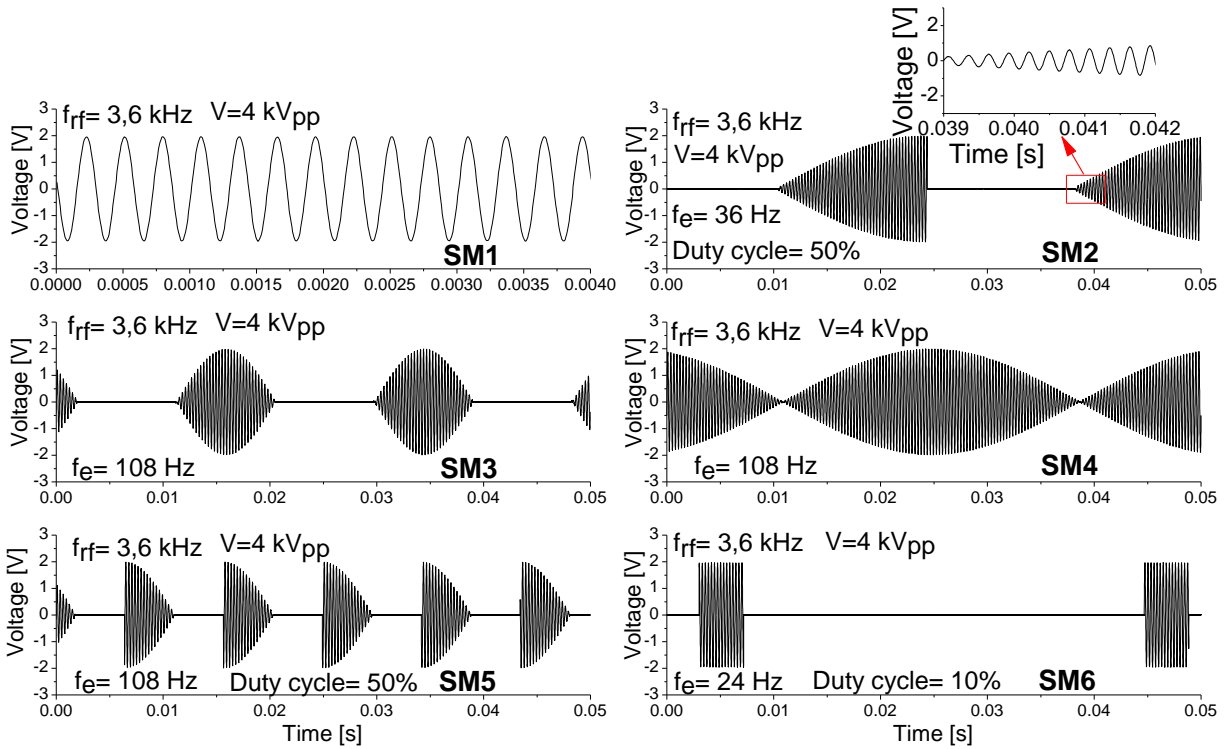


Figure 5. Plot of modulated signals to apply DBD plasma actuator.

RESULTS

The effectiveness of the DBD plasma actuator for flow separation control and lift augmentation is experimentally examined by using the force measurement system. Figure 6 (a) indicates lift coefficient variation as a function of attack angle and lift

coefficient of the flat plate represented as $2\pi\alpha$. In this figure, the result of the present study performed at $Re = 4.5 \times 10^4$ is comparable with that of Asada *et al.* (2009) performed at $Re = 4.4 \times 10^4$. The present study shows reasonably similar trends with the results of Asada *et al.* (2009) but there is a little difference in the values. These differences could ascribe to calculation of the lift

coefficients from the surface pressure measurement data around the airfoil. Stall occurs after $\alpha = 10^\circ$ for both studies. It was indicated by Genç *et al.* (2012), Lissaman (1983) and Tani (1964) that stall at such a small attack angle could be the laminar separation bubble which is known to occur as an adverse pressure gradient between the laminar and turbulent reattachment region.

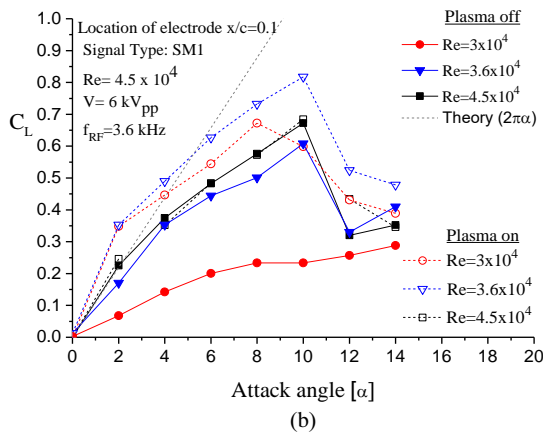
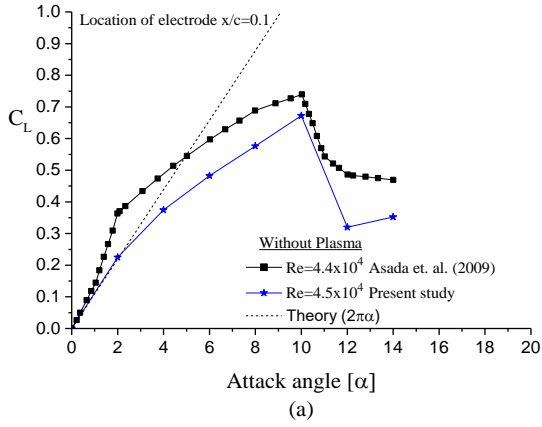


Figure 6. Variation of the mean lift coefficient as a function of angle of attack at (a) present study compared with Asada *et al.* (2009) and (b) different Re for plasma on and off.

Figure 6 (b) shows the variation of the lift coefficient as a function of attack angle by using a DBD plasma actuator with a driving SM1 type signal for $V = 6 \text{ kV}_{pp}$ and $f_{RF} 3.6 \text{ kHz}$ at $Re = 3 \times 10^4$, 3.6×10^4 and 4.5×10^4 . At $Re = 3 \times 10^4$ and 3.6×10^4 , the DBD plasma actuator significantly enhance the whole lift characteristics of the airfoil. The DBD plasma actuator producing an induced flow inside the boundary layer, adds momentum to the boundary layer (Benard and Moreau 2011; Esfahani *et al.* 2016). Therefore the separated shear layer is close to the surface of the airfoil and lift enhancement occurs. But the stall angle does not change for $V = 6 \text{ kV}_{pp}$ due to a strong adverse pressure gradient on the suction surface of the airfoil. While the actuator enhances the lift characteristics of the airfoil at $Re = 3 \times 10^4$ and 3.6×10^4 , there is no change in lift characteristics at $Re = 4.5 \times 10^4$. In such a high Reynolds number, induced flow generated by the DBD plasma actuator does not perturb the flow for $V = 6 \text{ kV}_{pp}$.

Drag coefficient results for 3.6×10^4 in the case of plasma on/off are given in figure 7 (a). As shown in this figure, there is no effect of the DBD plasma actuator on the drag coefficient. Therefore the drag coefficient results will not be presented in the following result sections. Aerodynamic efficiency ratio (C_L/C_D) as a function of attack angle is presented in figure 7 (b) for $Re = 3.6 \times 10^4$. Aerodynamic efficiency is significantly increased by the DBD plasma actuator. For the signal modulation given in Figure 11 and 12, experiments were carried out at $\alpha = 10^\circ$ because the lift curve for signal modulation was expected to show a more or less similar trend with figure 7(a).

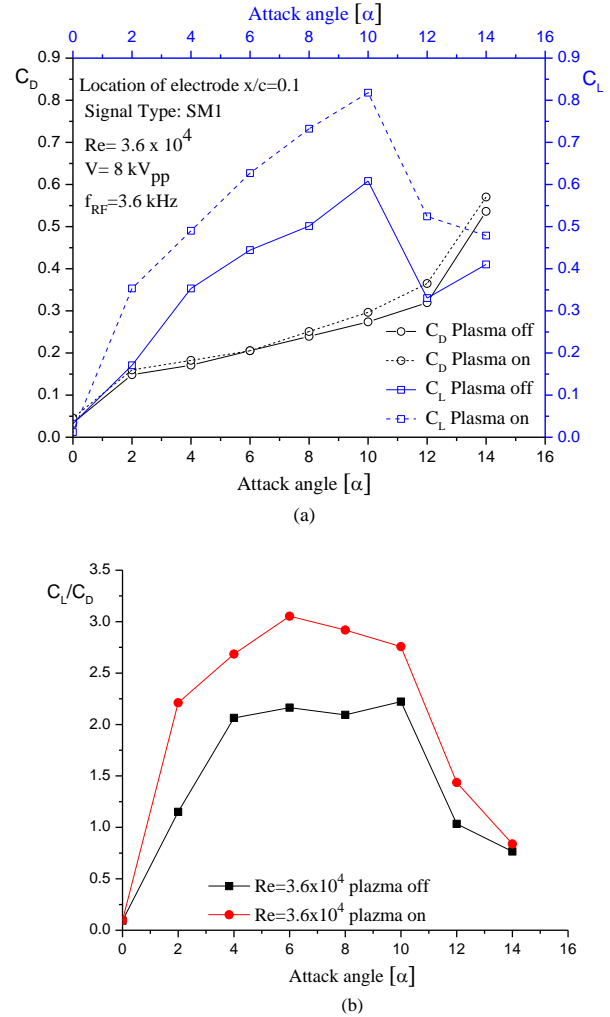


Figure 7. Variation of (a) the mean lift and drag coefficient, and (b) C_L/C_D as a function of angle of attack at $Re = 3.6 \times 10^4$.

Figure 8 shows a change in the mean lift coefficient versus Reynolds number (between 9.58×10^3 and 7.5×10^4) for different driving voltages which are 4, 6 and 8 kV_{pp} . SM1 is used as an actuator driving signal having a frequency of 3.6 kHz . It can be seen from these plots that there is a Reynolds number independence depending on plasma on/off situation due to the nearly constant lift coefficient for specific Reynolds number range.

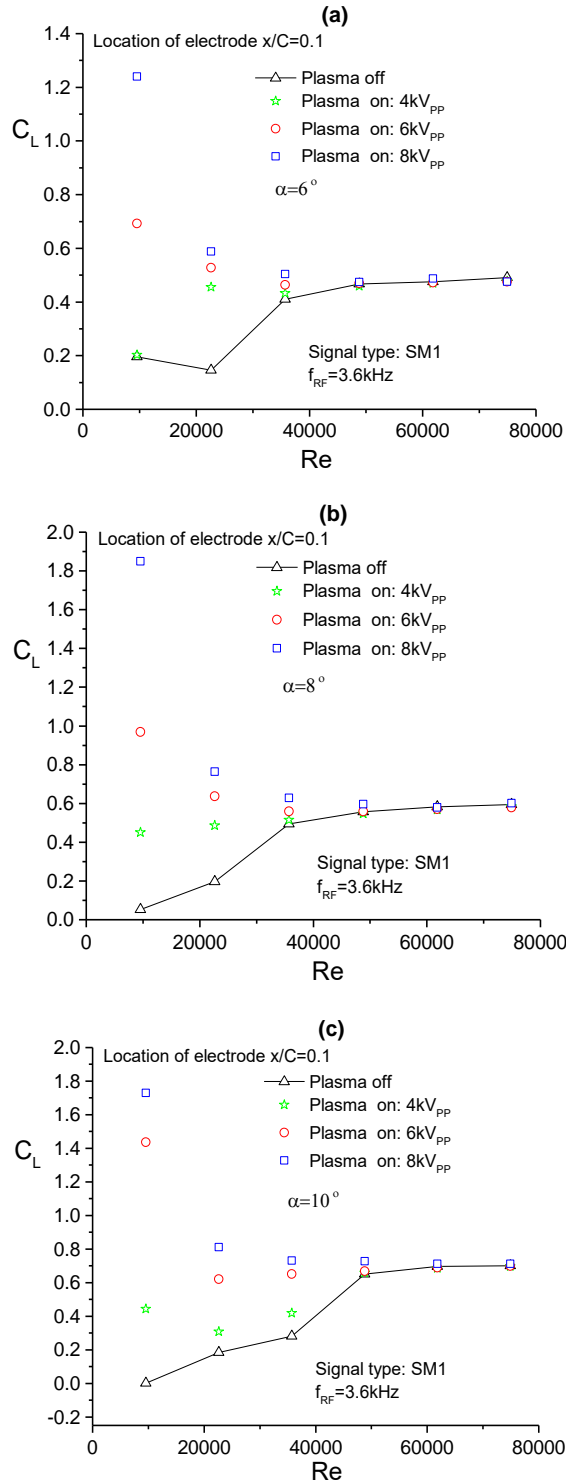


Figure 8. The mean lift coefficient versus Reynolds number (a) at 6° , (b) 8° and (c) 10° for different driving voltage.

It can be concluded from figure 8a and b that the lift coefficient is independent of Reynolds number between $Re = 3.6 \times 10^4$ and 7.5×10^4 at $\alpha = 6^\circ$ and 8° , for the plasma on/off situation. Also, the plasma actuator has the best effect with respect to lift augmentation when $Re < 3.6 \times 10^4$. Figure 8c indicates that the driving voltage of the plasma actuator or even the case without plasma has no effect on the lift coefficient because of roughly constant lift coefficient between $Re = 4.8 \times 10^4$ and 7.5×10^4 at the stall angle of 10° . As the driving voltage

increases at $Re < 4.8 \times 10^4$, the plasma actuator is more effective. Until now these experiments were carried out to determine stall angle and effective region of the actuator. The following experiments with the actuator were implemented to investigate whether the actuator can cope with the stall effect at $\alpha = 10^\circ$ or not. More extensive experiments shown in figure 9 were performed at $Re = 3 \times 10^4$ in order to show the effect of driving voltage and frequency at such a low Reynolds numbers.

Effects of variation of the driving voltage and the frequency on the improvement of the lift coefficient at $\alpha = 10^\circ$ are presented for a Reynolds number of 3×10^4 in figure 9. The change in lift coefficient versus driving voltage for $f_{RF} = 3.6$ kHz is represented by a red line. The change in lift coefficient versus RF frequency for $V = 6$ kV_{pp} is represented by the blue line. Effects of the driving voltage and frequency are clearly seen in this plot. When driving voltage is increased from 2 kV_{pp} to 8 kV_{pp} in $f_{RF} = 3.6$ kHz, the lift coefficient is significantly augmented from $C_L = 0.22$ to 0.79. Augmentation of the lift coefficient is also obtained by increasing the driving frequency from 2 kHz to 6 kHz with a constant driving voltage of 6 kV_{pp}. When these results are compared with the plasma off situation, maximum lift augmentation for the driving voltage and frequency is obtained as 259% and 245% respectively. There is no effect of the driving voltage on the lift augmentation until 2.5 kV_{pp}. As shown in this figure, lift coefficient is proportional to driving voltage and frequency due to increasing induced flow. These results support the results of Corke et al. (2010) and Giepmans and Kotsonis (2011). Lift coefficient curves are likely to be relatively in proportion to the variation of driving frequency and voltage.

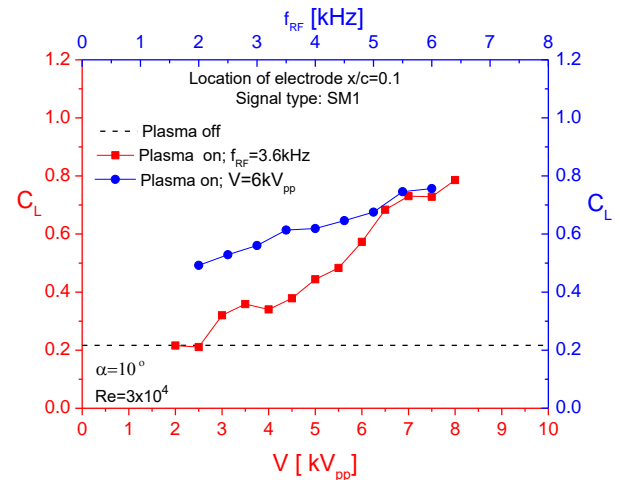


Figure 9. Change in lift coefficient based on driving voltage and RF frequency.

Smoke wire flow visualization results for different driving voltages of the DBD plasma actuator around NACA0015 airfoil at $\alpha = 10^\circ$ and $Re = 3 \times 10^4$ is presented in figure 10. For the case of actuator off, flow separation occurs at the leading edge of the airfoil and also a laminar bubble arises on the suction surface of the airfoil. For the case with actuator on, the wake region is narrow with the help of DBD plasma actuator adding momentum inside

the boundary layer at a driving voltage of 6 kV_{pp}. The wake region at V = 7 kV_{pp} is narrower than that at V = 6 kV_{pp}. This is attributed to pressure recovery on the suction surface (Post and Corke 2004) and increase in induced velocity as shown in figure 9. The narrowest wake width is obtained at V = 8 kV_{pp}. The flow visualization results indicated that increase in the lift coefficient is gradually augmented with increasing driving voltage from 6 kV_{pp} to 8 kV_{pp} due to gradually decreasing wake width of the airfoil. These results also support the results of Asada *et al.* (2009).

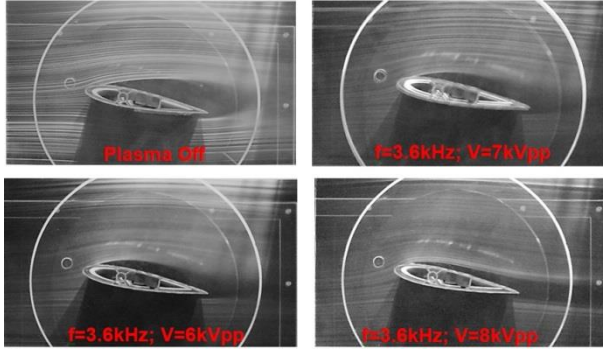


Figure 10. Effect of driving voltage of the DBD plasma actuator around NACA0015 airfoil at $\alpha = 10^\circ$ and $Re = 3 \times 10^4$.

Figure 11 shows the effects of excitation frequency, changing between 36 Hz and 360 Hz with an increment of 36 Hz, on the lift coefficient at different signal modulations with a driving voltage of 8 kV_{pp}. SM4 with regard to the flow separation control at $\alpha = 10^\circ$ is more effective than that of the other signal modulations, except for SM1 having a continuous sinusoidal signal. Generally, SM2, SM3, SM4 and SM5 have a lower effect than that of SM1 but they are at least 1.8 times more effective than that of the plasma off situation. In $f_e = 36, 108$ and 216 Hz, SM4 and SM1 have the same value of C_L and this can provide nearly 50% energy savings. These results show from figure 11 that there is a significant energy reduction and at least 80% lift augmentation for all f_e as compared to SM1.

Figure 12 shows the effects of the duty cycle changing between 1% and 99% on the lift coefficient for $F^+ = 0.2, 1, 1.3, 1.5$ and 3.7 with $V = 8$ kV_{pp} and $f_{RF} = 3.6$ kHz at $Re = 3.6 \times 10^4$. SM6 is given as an example signal type. In $F^+ = 1$, lift augmentation and effectiveness of the stall control have a better effect in comparison with the other F^+ in almost all duty cycles. It is noted that the lift coefficient produced by the DBD plasma actuator is strongly independent of F^+ for high duty cycles because the difference in the lift coefficient, when F^+ increases, is decreased by increasing duty cycle from 1% to 99%. By comparison with SM1, effects of the duty cycle for different F^+ increase by the augmenting duty cycle. At the 99% duty cycle, the lift coefficient of all F^+ is the same with SM1.

Minimum lift augmentation (64%) is obtained at a duty cycle of 1%. In lower duty cycle, DBD plasma actuator energy consumption gradually decreases (Daud *et al.* 2015; Mohammadi and Taleghani 2013; Moreau *et al.* 2016). As aforesaid in the introduction section, there are

two different results concerning the effect of dimensionless excitation frequency in the literature. Therefore, the present study has investigated the effect of F^+ with the change in duty cycle. Best lift augmentation is obtained in $F^+ = 1$ at the low duty cycle. This result is in good agreement with findings of Taleghani *et al.* (2012), Patel *et al.* (2008) and Göksel *et al.* (2007). This conflict in literature could be attributed to the different airfoil profiles, Reynolds number, actuator position, driving voltages and frequencies. While duty cycle increases, not only the differences in lift coefficient for all F^+ values decreases but also the lift coefficient increases for all F^+ values.

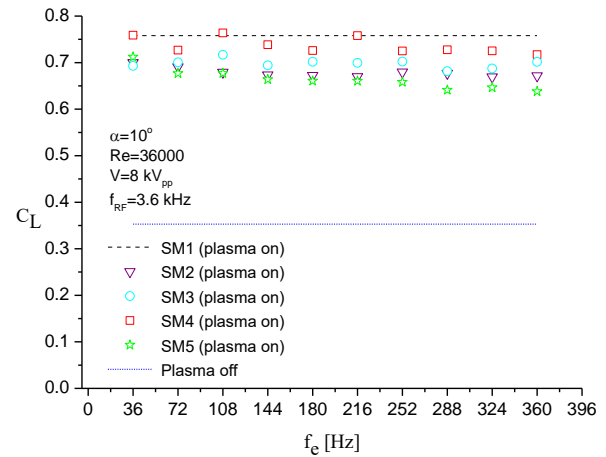


Figure 11. Effect of the variation of excitation frequency on the lift coefficient at different signal modulation.

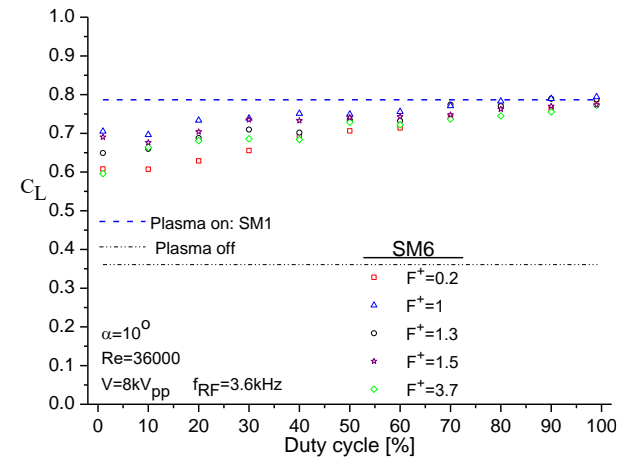


Figure 12. Effect of the duty cycle on the lift coefficient at different F^+ .

CONCLUSIONS

A parametric study is performed to determine the most effective measuring parameter by measuring lift acting on an airfoil for a wide range of Reynolds numbers and three different driving voltages. The efficiency of the actuator on the stall control is investigated experimentally using different modulated signals at an attack angle of 10° . In addition, the effects of the duty cycle, the amplitude modulation and the excitation frequency on the flow separation point are presented. It

is found that the actuator with the driving voltages of 6 kV_{pp} and 8 kV_{pp} has a better effect for Reynolds number between 9.5×10^3 and 4.8×10^4 at $\alpha=10^\circ$. The flow visualization results indicate that a gradual increase in the lift coefficient is obtained with increasing driving voltage from 6 kV_{pp} to 8 kV_{pp} due to gradually decreasing wake width of the airfoil. The lift augmentation was obtained both by increasing the f_{RF} from 2 kHz to 6 kHz for the constant driving voltage of 6 kV_{pp} and by increasing the driving voltage from 2.5 kV_{pp} to 8 kV_{pp} for the constant $f_{RF} = 3.6$ kHz. SM4 including amplitude modulation on lift augmentation has a better effect than that of the other modulated signals (SM2, SM3 and SM5) at $Re = 3.6 \times 10^4$ and also has nearly the same effect with the SM1 signal. All modulation signals are at least 1.8 times more effective than the plasma off situation. For the separation control, the applied different modulated signals consume less energy than the continuous sinusoidal signal.

ACKNOWLEDGEMENTS

The authors would like to acknowledge the financial support of this work by the Scientific and Technological Research Council of Turkey (TUBITAK) under the Contract Number of 110M056. The authors also thank the rest of project team for their assistance in the performing of the study.

REFERENCES

- Akansu, Y. E., Bayindirli, C. and Seyhan, M., 2016, The Improvement of Drag Force on a Truck Trailer Vehicle By Passive Flow Control Methods, *Isı Bilimi ve Tekniği Dergisi-Journal Of Thermal Science And Technology*, 36(1), 133–141.
- Akansu, Y. E., Karakaya, F. and Şanlısoy, A., 2013, Active Control of Flow around NACA 0015 Airfoil by Using DBD Plasma Actuator., *EPJ Web of Conferences*, 45, 1008.
- Akansu, Y. E., Sarioglu, M. and Yavuz, T., 2004, Flow around a Rotatable Circular Cylinder-Plate Body at Subcritical Reynolds Numbers, *AIAA Journal*, 42(6), 1073–1080.
- Akbıyık, H., Akansu, Y. E. and Yavuz, H., 2017, Active Control of Flow around a Circular Cylinder By Using Intermittent DBD Plasma Actuators, *Flow Measurement and Instrumentation*, 53, 215–220.
- Asada, K., Ninomiya, Y., Oyama, A. and Fujii, K., 2009, Airfoil Flow Experiment on the Duty Cycle of DBD Plasma Actuator, *47th AIAA Aerospace Sciences Meeting including The New Horizons Forum and Aerospace Exposition*.
- Benard, N. and Moreau, E., 2011, On the Vortex Dynamic of Airflow Reattachment Forced by a Single Non-thermal Plasma Discharge Actuator. *Flow, Turbulence and Combustion*, 87(1), 1–31.
- Benard, N. and Moreau, E., 2013, Response of a Circular Cylinder Wake to a Symmetric Actuation By Non-Thermal Plasma Discharges, *Experiments in Fluids*, 54(2), 1467.
- Benard, N. and Moreau, E., 2014, Electrical and Mechanical Characteristics of Surface AC Dielectric Barrier Discharge Plasma Actuators Applied to Airflow Control, *Experiments in Fluids*, 55(11), 1846.
- Coleman, H. W. and Steele, W. G., 2009, *Experimentation, Validation, and Uncertainty Analysis for Engineers*, John Wiley & Sons.
- Corke, Thomas C., Enloe and Lon C., 2010, Dielectric Barrier Discharge Plasma Actuators for Flow Control, *Annual Review of Fluid Mechanics*, 42(1), 505–529.
- Corke, T. C., Post, M. L. and Orlov, D. M., 2009, Single Dielectric Barrier Discharge Plasma Enhanced Aerodynamics: Physics, Modeling and Applications. *Experiments in Fluids*, 46(1), 1–26.
- De Giorgi, M. G., Ficarella, A., Marra, F. and Pescini, E., 2017, Micro DBD Plasma Actuators for Flow Separation Control on a Low Pressure Turbine at High Altitude Flight Operating Conditions of Aircraft Engines, *Applied Thermal Engineering*, 114, 511–522.
- Esfahani, A., Singhal, A., Clifford, C. J. and Samimy, M., 2016, Flow Separation Control over a Boeing Vertol VR-7 using NS-DBD Plasma Actuators, *54th AIAA Aerospace Sciences Meeting*, (January), 1–17.
- Feng, L. H., Jukes, T. N., Choi, K. S. and Wang, J. J., 2012, Flow Control over a NACA 0012 Airfoil using Dielectric Barrier Discharge Plasma Actuator with a Gurney Flap, *Experiments in Fluids*, 52(6), 1533–1546.
- Forte, M., Jolibois, J., Pons, J., Moreau, E., Touchard, G. and Cazalens, M., 2007, Optimization of a Dielectric Barrier Discharge Actuator by Stationary and Non-Stationary Measurements of the Induced Flow velocity: Application to Airflow Control, *Experiments in Fluids*, 43(6), 917–928.
- Genç, M. S., Karasu, I. and Hakan Açikel, H., 2012, An Experimental Study on Aerodynamics of NACA2415 Aerofoil at Low Re Numbers, *Experimental Thermal and Fluid Science*, 39, 252–264.
- Giepmans, R. H. M. and Kotsonis, M., 2011, On the Mechanical Efficiency of Dielectric Barrier Discharge Plasma Actuators, *Applied Physics Letters*, 98(22), 130–132.
- Göksel, B., Greenblatt, D., Rechenberg, I., Bannasch, R. and Paschereit, C. O., 2007, Plasma Flow Control at MAV Reynolds Numbers. *3rd US-European Competition and Workshop on Micro Air Vehicle Systems (MAV07) & European Micro Air Vehicle Conference and Flight Competition (EMAV2007)*, 71–76.

- Göksel, B., Greenblatt, D., Rechenberg, I., Kastantin, Y., Nayeri, C. N. and Paschereit, C. O., 2007, Pulsed Plasma Actuators for Active Flow Control at MAV Reynolds Numbers, *Active Flow Control*, 42–55, Springer.
- Greenblatt, D., Kastantin, Y., Nayeri, C. N. and Paschereit, C. O., 2008, Delta-wing Flow Control Using Dielectric Barrier Discharge Actuators. *AIAA journal*, 46(6), 1554–1560.
- Huang, J., Corke, T. C. and Thomas, F. O., 2006, Plasma Actuators for Separation Control of Low-Pressure Turbine Blades, *AIAA Journal*, 44(1), 51–57.
- Ibrahimoglu, B., Yilmazoglu, M. Z. and Cücen, A., 2016, Numerical Analysis of Active Control of Flow on a DBD Plasma Actuator Integrated Airfoil, *Sustainable Aviation*, 363–374, Springer.
- Jukes, T., Segawa, T., Walker, S., Furutani, H., Iki, N. and Takekawa, S., 2012, Active Separation Control over a NACA0024 by DBD Plasma Actuator and FBG Sensor. *Journal of Fluid Science and Technology*, 7(1), 39–52.
- Lissaman, P. B. S. (1983). Low-Reynolds-Number Airfoils. *Ann. Rev. Fluid Mech*, 15, 223–39.
- Little, J., Nishihara, M., Adamovich, I. and Samimy, M., 2010, High-lift airfoil trailing edge separation control using a single dielectric barrier discharge plasma actuator, *Experiments in fluids*, 48(3), 521–537.
- Md Daud, N., Kozato, Y., Kikuchi, S. and Imao, S., 2015, Control of leading edge separation on airfoil using DBD plasma actuator with signal amplitude modulation. *Journal of Visualization*, 19(1), 37–47.
- Menghu, H., Jun, L., Zhongguo, N., Hua, L., Guangyin, Z. and Weizhuo, H., 2015, Aerodynamic performance enhancement of a flying wing using nanosecond pulsed DBD plasma actuator, *Chinese Journal of Aeronautics*, 28(2), 377–384.
- Mohammadi, M. and Taleghani, A. S., 2013, Active Flow Control by Dielectric Barrier Discharge to Increase Stall Angle of a NACA0012 Airfoil, *Arabian Journal for Science and Eng.*, 39(3), 2363–2370.
- Moreau, E., 2007, Airflow control by non-thermal plasma actuators, *Journal of Physics D: Applied Physics*, 40, 605–636.
- Moreau, E., Debien, A., Breux, J. M., & Benard, N. (2016). Control of a turbulent flow separated at mid-chord along an airfoil with DBD plasma actuators. *Journal of Electrostatics*, 83, 78–87.
- Nelson, R., Corke, T., He, C., Othman, H., Matsuno, T., Patel, M., and Ng, T., 2007, Modification of the Flow Structure over a UAV Wing for Roll Control, *45th AIAA Aerospace Sciences Meeting and Exhibit*, (January), 1–15.
- Patel, M. P., Ng, T. T., Vasudevan, S., Corke, T. C. and He, C., 2007, Plasma Actuators for Hingeless Aerodynamic Control of an Unmanned Air Vehicle, *Journal of Aircraft*, 44(4), 1264–1274.
- Patel, M. P., Ng, T. T., Vasudevan, S., Corke, T. C., Post, M., McLaughlin, T. E. and Suchomel, C. F., 2008, Scaling effects of an aerodynamic plasma actuator. *Journal of aircraft*, 45(1), 223–236.
- Pescini, E., Marra, F., De Giorgi, M. G., Francioso, L., and Ficarella, A., 2017, Investigation of the boundary layer characteristics for assessing the DBD plasma actuator control of the separated flow at low Reynolds numbers, *Experimental Thermal and Fluid Science*, 81, 482–498.
- Post, M. L. and Corke, T. C., 2004, Separation Control on High Angle of Attack Airfoil Using Plasma Actuators, *AIAA Journal*, 42(11), 2177–2184.
- Roth, J. R., 2003, Aerodynamic flow acceleration using paraelectric and peristaltic electrohydrodynamic effects of a one atmosphere uniform glow discharge plasma, *Physics of Plasmas (1994-present)*, 10(5), 2117–2126.
- Rudmin, D., Benaissa, A. and Poirel, D., 2013, Detection of Laminar Flow Separation and Transition on a NACA-0012 Airfoil Using Surface Hot-Films *Journal of Fluids Engineering*, 135(10), 101104.
- Sarioglu, M. (2017). Control of flow around a square cylinder at incidence by using a splitter plate. *Flow Measurement and Instrumentation*, 53, 221–229.
- Sarioglu, M., Akansu, Y. E. and Yavuz, T., 2005, Control of flow around square cylinders at incidence by using a rod, *AIAA Journal*, 43(7), 1419–1426.
- Sarioglu, M., Akansu, Y. E. and Yavuz, T., 2006, Flow Around a Rotatable Square Cylinder-Plate Body, *AIAA Journal*, 44(5), 1065–1072.
- Sosa, R. and Artana, G. (2006). Steady control of laminar separation over airfoils with plasma sheet actuators. *Journal of Electrostatics*, 64(7–9), 604–610.
- Taleghani, A. S., Shadaram, A. and Mirzaei, M., 2012, Effects of duty cycles of the plasma actuators on improvement of pressure distribution above a NLF0414 airfoil, *Plasma Science, IEEE Transactions on*, 40(5), 1434–1440.
- Tani, I., 1964, Low-speed flows involving bubble separations, *Progress in Aerospace Sciences*, 5, 70–103.
- Thomas, F. O., Kozlov, A. and Corke, T. C., 2008, Plasma Actuators for Cylinder Flow Control and Noise Reduction, *AIAA Journal*, 46(8), 1921–1931.
- Wang, J. J., Choi, K. S., Feng, L. H., Jukes, T. N. and Whalley, R. D., 2013, Recent developments in DBD plasma flow control, *Progress in Aerospace Sciences*, 62, 52–78.



Adem Arif GÜLER received his B.Sc. degree Mechanical Engineering department from Erciyes University in 2008 and M.sc degree in Mechanical Engineering department from Niğde Ömer Halisdemir University in 2013. He is currently working as machine supply and operation engineer in Niğde Special Provincial Administration.



Mehmet SEYHAN, received his B.Sc. degree and M.Sc. degree in Mechanical Engineering from Niğde University in 2013 and 2015, respectively. He is currently a PhD student at Karadeniz Technical University, where he also works as research assistant. His research interests include plasma actuators for flow control, PEM fuel cells and flow control applications.



Yahya Erkan AKANSU, received his B.Sc. degree in Mechanical Engineering from Erciyes University in 1993, M.Sc. degree and Ph.D. degree from Karadeniz Technical University in 1998 and 2004, respectively. He currently works as Professor in Mechanical Engineering Department of Niğde Ömer Halisdemir University. His research interests include active and passive aerodynamic flow control applications.